

Analysis of 3D wall building structures dynamic response

T. Chyzy[†], J. Kretowska[‡] and Cz. Miedzialowski^{‡†}

Department of Civil Engineering, Bialystok University of Technology,
ul. Wiejska 45E, 15-351 Bialystok, Poland

(Received March 24, 2005, Accepted October 11, 2005)

Abstract. Three-dimensional description of building structure taking into consideration soil-structure interaction is a very complex problem and solution of this problem is often obtained by using finite element method. However, this method takes a significant amount of computational time and memory. Therefore, an efficient computational model based on subdivision of the structure into building elements such as wall and floor slab elements, plane and three-dimensional joints and lintels, that could provide accurate results with significantly reduced computational time, is proposed in this study for the analysis three-dimensional structures subjected to dynamic load. The examples prove the efficiency and the computing possibilities of the model.

Key words: three-dimensional building elements; super elements; dynamic problem formulation; finite element method.

1. Introduction

Building supporting structures are often exposed to changing load such as changing wind pressure or displacements of building footing caused by seismic movements of the earth's crust (seismic effects), by roiling stocks and roads vibrations (paraseismic effects) or by vibrations of local sources and explosions. Additionally, in concrete structures, not only structural members of the building but also joints are flexible to plasticizing and cracking. These various effects cause changes of stiffness of elements and changes of a structure response to acting load.

Many building structures are constructed using coupled shear walls or shear wall-frame systems. Therefore, much research on efficient analysis of such structures has been undertaken (Kim and Lee 2002, 2005). Plane stress elements and beam elements have been used to model the shear wall core and frames. The transition region in which beam and shear walls or frames are interconnected is often the weakest area. In general, wall element is treated in FEM as plane stress element (has two translational degrees of freedom per node) and beam element has three degree of freedom per node (two translational and one rotational). Due to this reason, much research workers have taken into account the connections between shear wall and beam or shear wall and frame (Thomas 1989, Kim and Hong 1995, Choi *et al.* 1996, 1998, 1999). Shear walls may have openings for functional

[†] Ph.D., E-mail: teddy@pb.bialystok.pl

[‡] Ph.D., Corresponding author, E-mail: J.Kretowska@kmb.pb.bialystok.pl

^{‡†} Professor, E-mail: cz.miedzialowski@kmb.pb.bialystok.pl

reason. The location, number and size of openings affects the structure behaviour. Therefore, the analysis of such a type of elements have been undertaken by Ali and Atwall (1980), Choi and Bang (1987).

Three-dimensional finite element model of building structure, which takes into consideration joints and soil foundation is necessary for an accurate analysis. However, such a model and “step by step” method of computation take a significant amount of computational time and memory. Therefore super elements have been employed by research workers to describe building structure elements (Kim *et al.* 2003) what drastically reduced computational time and memory.

The paper presents an efficient computational model (called MQDES) based on subdivision of the structure into building elements such as wall and floor slab elements, plane and three-dimensional joints and lintels, that could provide accurate results with significantly reduced computational time. The theory of Timoshenko-type beam has been used to describe wall and floor strips but the compression and twisting have been added to the classical formulation. The proposed description allows to obtain internal forces for every strip what can be very useful in the engineering practice (designing process).

Proposed model can be useful for the analysis of three-dimensional structures subjected to dynamic and static loads but especially for the analysis of building structures, where mainly walls are responsible for the stiffness of the building.

2. The computational model

2.1 The model formulation

The computational model is formulated on the basis of the finite element method in agreement with Zienkiewicz (1986). The discrete model is constructed using the subdivision of the structure into building elements such as wall and floor slab elements, plane and three-dimensional joints (vertical and horizontal) and lintels (Miedzialowski 1995), Fig. 1. Wall and floor elements (Fig. 2a),

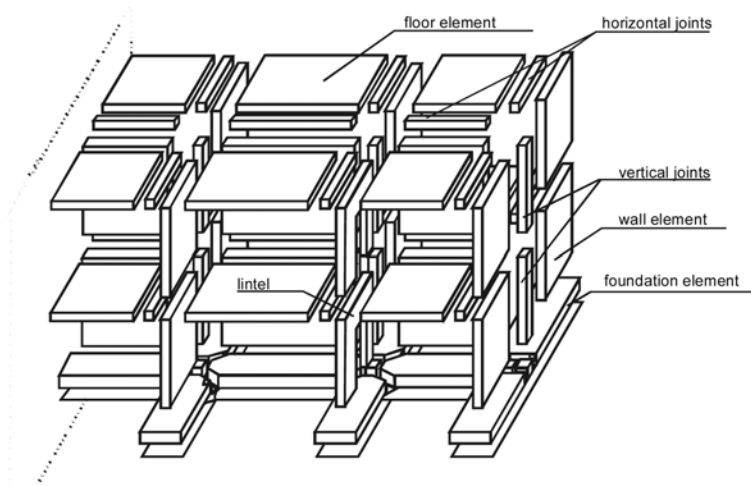


Fig. 1 The subdivision of the structure into building elements

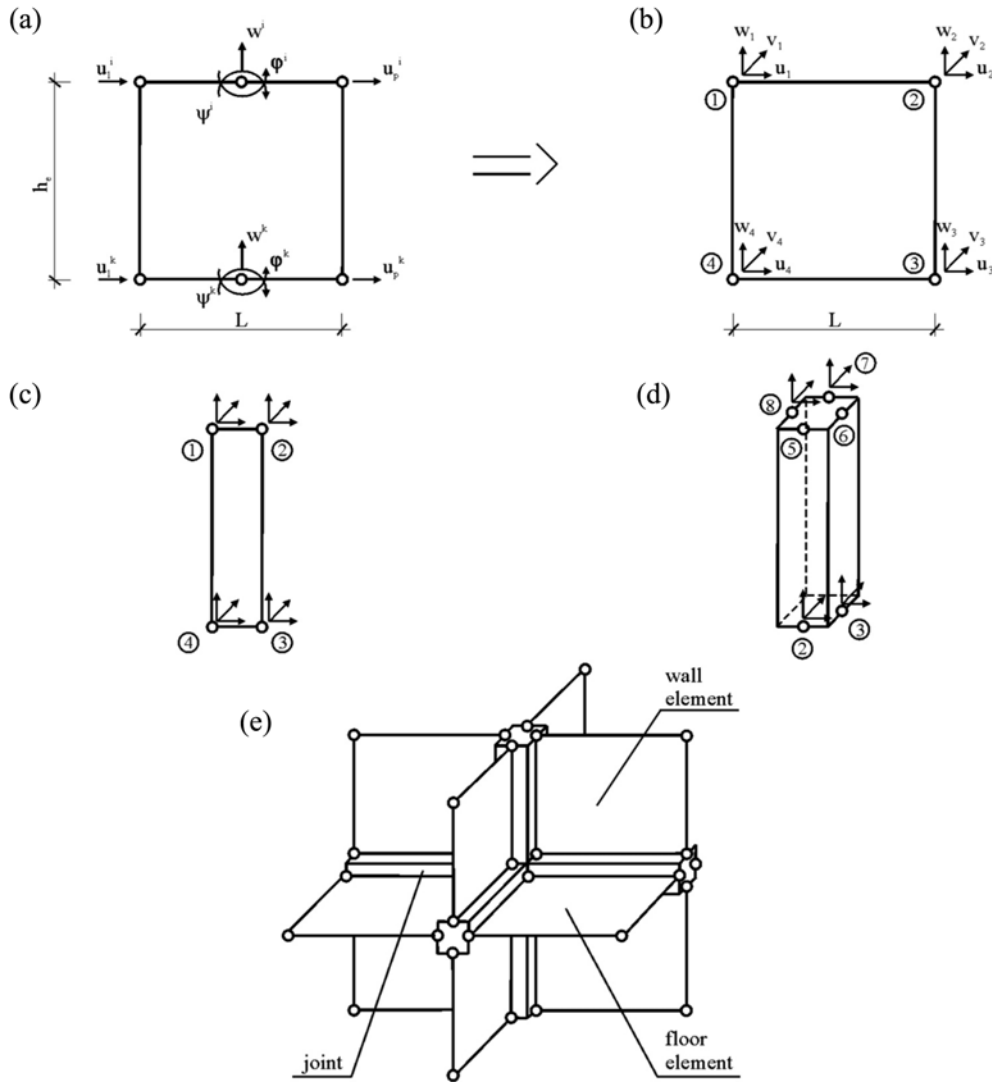


Fig. 2 Elements of the computational model

which are treated as vertical and horizontal strips, are described by deep beam scheme taking into account compression and twisting. Transverse section deformation is assumed as in Timoshenko-type beam in agreement with Timoshenko and Goodier (1951) and Rakowski (1990).

The displacement field of wall and floor strips is expressed by

$$\mathbf{f}_w = \begin{Bmatrix} u \\ v \\ w \end{Bmatrix} = \begin{Bmatrix} u \\ 0 \\ w_0 \end{Bmatrix} + \begin{Bmatrix} 0 \\ x\psi \\ -x\varphi \end{Bmatrix} \quad (1)$$

where:

- φ - angle of rotation of the strip cross-section,
- ψ - angle of twist of the strip cross-section.

The strain field is written as

$$\boldsymbol{\varepsilon}_w = \begin{Bmatrix} \varepsilon_x \\ \varepsilon_z \\ \gamma_{zx} \\ \gamma_{zx}^s \end{Bmatrix} = \begin{Bmatrix} \frac{u_l - u_p}{L} \\ \frac{\partial w}{\partial z} \\ \frac{\partial w}{\partial x} + \frac{\partial y}{\partial z} \\ 2y \frac{\partial \psi}{\partial z} \end{Bmatrix} = \begin{Bmatrix} \frac{u_l - u_p}{L} \\ \frac{\partial w_0}{\partial z} - x \frac{\partial \varphi}{\partial z} \\ -\varphi + \frac{\partial(u_l + u_p)}{2\partial z} \\ 2y \frac{\partial \psi}{\partial z} \end{Bmatrix} \quad (2)$$

where:

- l, p - two adjacent points between which strain is averaged,
- L - distance between points l and p (width of the strip).

The strain vector has the form

$$\boldsymbol{\varepsilon}_w = \mathbf{L} \bar{\mathbf{f}}_w \quad (3)$$

where:

$$\mathbf{L} = \begin{bmatrix} \frac{1}{L} & -\frac{1}{L} & 0 & 0 & 0 \\ 0 & 0 & \frac{\partial}{\partial z} & -x \frac{\partial}{\partial z} & 0 \\ \frac{\partial}{2\partial z} & \frac{\partial}{2\partial z} & 0 & -1 & 0 \\ 0 & 0 & 0 & 0 & 2y \frac{\partial}{\partial z} \end{bmatrix} \quad (4)$$

$$\bar{\mathbf{f}}_w = \{u_l \ u_p \ w_0 \ \varphi \ \psi\}^T \quad (5)$$

The stress field is determined as follows:

$$\boldsymbol{\sigma} = \mathbf{D} \boldsymbol{\varepsilon} = \mathbf{D} \mathbf{L} \bar{\mathbf{f}}_w \quad (6)$$

where:

\mathbf{D} - constitutive matrix.

Plane and spatial joints are placed between floor and wall strips.

The displacement field in the plane joints (Fig. 2c) can be expressed by:

$$\mathbf{f}_j = \begin{Bmatrix} u \\ v \\ w \end{Bmatrix} = \begin{Bmatrix} u \\ 0 \\ w_0 \end{Bmatrix} + \begin{Bmatrix} 0 \\ x\psi_r \\ -x\varphi_r \end{Bmatrix} \quad (7)$$

The strains can be calculated as follows:

$$\boldsymbol{\varepsilon}_j = \begin{Bmatrix} \varepsilon_x \\ \gamma_{xz} \\ \gamma_{zx}^s \end{Bmatrix} \quad (8)$$

where:

$$\varepsilon_x = \frac{(u_l - u_p)}{l_n} \quad (9)$$

$$\gamma_{xz} = -\varphi_r + \frac{\partial u}{\partial z} = \frac{1}{l_n}(w_l - w_p) + \frac{\partial(u_l - u_p)}{2\partial z} \quad (10)$$

$$\gamma_{zx}^s = 2y \frac{\partial \psi_r}{\partial z} = 2y \frac{\partial(u_l - u_p)}{l_n \partial z} \quad (11)$$

where:

- φ_r - angle of rotation of the plane joint cross-section,
- ψ_r - angle of twist of the plane joint cross-section,
- l_n - width of the joint.

Lintel strips, which have deep beam proportions in wall structures, are modelled as uniformly distributed wall connections taking into consideration bending effects.

Therefore, the modulus of elasticity in the model of plane joint are modified according to the following expression

$$G = \frac{Cl_n}{h_{vz}} \quad (12)$$

where:

- h_{vz} - thickness of the adjacent walls,
- $C = T/\delta$ - stiffness of the joint, which is calculated as

$$C = \frac{1}{\left(\frac{l_{n0}^3}{12E_{bn}J_n} + \frac{l_{n0}}{G_{bn}F_n} \right) h_k} \quad (13)$$

where:

- T - shear force per unit length of the joint,
- δ - displacement of joint edges,
- l_{n0} - reduced joint length,

$$l_{no} = l_n + (0.3 \div 0.5)h_n \quad (14)$$

h_n - lintel height,

F_n, I_n - cross-sectional area and moment of inertia of the lintel,

h_k - storey height.

Connection between three or four strips and two strips situated in a different plane is described by three-dimensional joint (Figs. 2d,e)

However, the displacement field of the spatial joints (Fig. 2d) is assumed as in three-dimensional state of stress.

$$f_j = \begin{Bmatrix} u \\ v \\ w \end{Bmatrix} = \begin{Bmatrix} u(x, y, z) \\ v(x, y, z) \\ w(x, y, z) \end{Bmatrix} \quad (15)$$

Strain field is calculated as

$$\boldsymbol{\varepsilon}_j = \begin{Bmatrix} \varepsilon_x \\ \varepsilon_y \\ \varepsilon_z \\ \gamma_{xy} \\ \gamma_{yz} \\ \gamma_{xz} \end{Bmatrix} = \begin{bmatrix} \frac{\partial}{\partial x} & 0 & 0 \\ 0 & \frac{\partial}{\partial y} & 0 \\ 0 & 0 & \frac{\partial}{\partial z} \\ \frac{\partial}{\partial y} & \frac{\partial}{\partial x} & 0 \\ 0 & \frac{\partial}{\partial x} & \frac{\partial}{\partial y} \\ \frac{\partial}{\partial z} & 0 & \frac{\partial}{\partial x} \end{bmatrix} \mathbf{f}_j = \mathbf{L}_j \mathbf{f}_j \quad (16)$$

Stress field can be described by

$$\boldsymbol{\sigma}_j = \mathbf{D} \boldsymbol{\varepsilon}_j = \mathbf{D} \mathbf{L}_j \mathbf{f}_j \quad (17)$$

where:

$$\mathbf{D} = \frac{E_j}{(1 + \nu)(1 - 2\nu)} (\mathbf{D}_{diag} + \mathbf{D}_{12}) \quad (18)$$

$$D_{diag} = \left[1 - \nu, \quad 1 - \nu, \quad 1 - \nu, \quad \frac{1 - 2\nu}{2}, \quad \frac{1 - 2\nu}{2}, \quad \frac{1 - 2\nu}{2} \right] \quad (19)$$

\mathbf{D}_{12} - matrix 6×6 in which: $d_{12} = d_{13} = d_{21} = d_{23} = d_{31} = d_{32} = \nu$ and the other elements are equal 0.

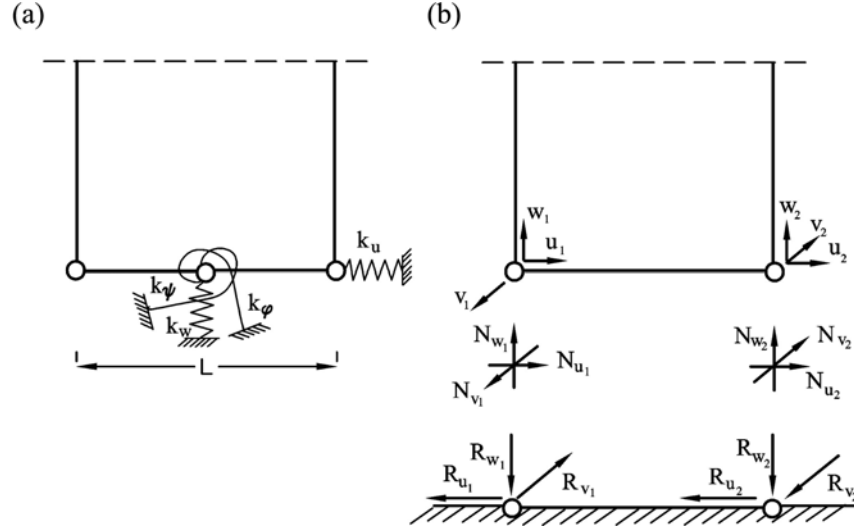


Fig. 3 The subsoil interaction in the contact model (a) Elastic constrains, (b) Soil-structure interaction

The subsoil is presented as contact model described by spring constraints (Fig. 3).

Taking into account structural elements, the displacements can be expressed as follows:

$$u_1 = u_1 \quad (20)$$

$$u_p = u_2 \quad (21)$$

$$w = \frac{w_1 + w_2}{2} \quad (22)$$

$$\varphi = \frac{w_1 - w_2}{L} \quad (23)$$

$$\psi = \frac{v_1 - v_2}{L} \quad (24)$$

2.2 The finite element method application

The solution of the problem using finite element method is reduced to a defined number of points, called nodes.

The unknown displacements distribution of wall and floor elements $\bar{\mathbf{f}}_w$ is expressed by:

$$\bar{\mathbf{f}}_w = \mathbf{N} \mathbf{d}_e \quad (25)$$

where, \mathbf{N} - shape function matrix.

\mathbf{d}_e - vector of unknown displacements at nodes of finite elements

$$\mathbf{d}_e = \{u_1^i \ u_p^i \ w^i \ \varphi^i \ \psi^i \ u_1^k \ u_p^k \ w^k \ \varphi^k \ \psi^k\}^T \quad (26)$$

The equation of virtual work in dynamic problem is given by

$$\int_t \left\{ \int_V [(\delta \boldsymbol{\varepsilon})^T \boldsymbol{\sigma} + (\delta \bar{\mathbf{f}})^T (c \dot{\bar{\mathbf{f}}} + \rho \ddot{\bar{\mathbf{f}}})] dV - \int_V (\delta \bar{\mathbf{f}})^T \mathbf{p}(\mathbf{t}) dV \right\} dt = 0 \quad (27)$$

where:

- c - damping parameter,
- ρ - mass parameter,
- $p(t)$ - changing load.

The Eq. (28), which is expressed by internal forces \mathbf{W} , has been obtained by using formulas (3) and (4) and by integration of the Eq. (27)

$$\int_t \left\{ \int_h [(\delta \bar{\mathbf{f}})^T \mathbf{L}^T \mathbf{W} + F(\delta \bar{\mathbf{f}})^T (c \dot{\bar{\mathbf{f}}} + \rho \ddot{\bar{\mathbf{f}}}) - F(\delta \bar{\mathbf{f}})^T \mathbf{p}(\mathbf{t})] dz \right\} dt = 0 \quad (28)$$

where:

- F - cross-sectional area.

$$\mathbf{W} = \{N_x \quad N_z \quad Q_{zx} \quad M_y \quad M_s\} \quad (29)$$

Internal forces can be obtained by using FEM

$$\mathbf{W} = \bar{\mathbf{D}} \mathbf{L} \bar{\mathbf{f}} = \bar{\mathbf{D}} \mathbf{L} \mathbf{N} \mathbf{d}_e = \bar{\mathbf{D}} \mathbf{B} \mathbf{d}_e \quad (30)$$

where:

- $\bar{\mathbf{D}}$ - constitutive matrix,
- \mathbf{N} - matrix of a shape function,
- \mathbf{d}_e - displacement vector of nodes.

Using Eq. (28) the typical system of differential equations can be obtained

$$\mathbf{M} \ddot{\mathbf{d}} + \mathbf{C} \dot{\mathbf{d}} + \mathbf{K} \mathbf{d} = \mathbf{P}(\mathbf{t}) \quad (31)$$

The solution of the Eq. (31) can be obtained by using one of well known numerical method i.e.: indirect method (reduction and modal superposition) or direct method (Newmark and finite-difference method).

The forces of subsoil interaction have the form:

$$\mathbf{K}_f \mathbf{d}_f = \mathbf{R}_f \quad (32)$$

where:

$$\mathbf{K}_f = \mathbf{K}_{f \text{diag}} + \mathbf{K}_{f12} \quad (33)$$

$$\mathbf{K}_{f \text{diag}} = [a \quad b_1 \quad -c \quad a \quad b_1 \quad -c] \quad (34)$$

$$\mathbf{d}_f = \{u_1 \quad w_1 \quad v_1 \quad u_2 \quad w_2 \quad v_2\}^T \quad (35)$$

$$\mathbf{R}_f = \{R_{u_1} \ R_{w_1} \ R_{v_1} \ R_{u_2} \ R_{w_2} \ R_{v_2}\}^T \quad (36)$$

where: \mathbf{R}_f - forces of subsoil interaction,

\mathbf{K}_{f12} - matrix 6×6 in which: $k_{25} = k_{52} = b_2$, $k_{36} = k_{63} = c$ and the other elements are equal 0.

$$a = \frac{1}{2} F_f k_u$$

$$b_1 = \frac{1}{4} F_f k_w + \frac{1}{L^2} J_f k_w$$

$$b_2 = \frac{1}{4} F_f k_w - \frac{1}{L^2} J_f k_w$$

$$c = \frac{1}{L^2} J_0 k_v$$

F_f, J_f, J_0 - cross-sectional area and moments of inertia of the foundation footing,
 k_u, k_v, k_w - proportional subsoil coefficients.

Taking into account the subsoil the computational model has a form:

$$\begin{bmatrix} \mathbf{M}_{11} & \\ & \mathbf{M}_{22} \end{bmatrix} \begin{Bmatrix} \ddot{\mathbf{u}}_k \\ \ddot{\mathbf{u}}_f \end{Bmatrix} + \begin{bmatrix} \mathbf{C}_{11} & \\ & \mathbf{C}_{22} \end{bmatrix} \begin{Bmatrix} \dot{\mathbf{u}}_k \\ \dot{\mathbf{u}}_f \end{Bmatrix} + \begin{bmatrix} \mathbf{K}_{11} & \mathbf{K}_{12} \\ \mathbf{K}_{21} & \mathbf{K}_{22} + \mathbf{K}_f \end{bmatrix} \begin{Bmatrix} \mathbf{u}_k \\ \mathbf{u}_f \end{Bmatrix} = \begin{Bmatrix} \mathbf{P}_k \\ \mathbf{P}_f \end{Bmatrix} \quad (37)$$

where, k - degree of freedom of the structure,

f - degree of freedom of the contact zone between structure and subsoil.

In order to enable easier implementation of connections of finite elements, according to presented model, the unknown displacements are transferred to the corners of elements (Fig. 2b).

Presented structural model requires the description of changes of stiffness at level of every element cross-section such as that of Miedzialowski (1995).

The continual method and the multistrip finite element method are used in the model description.

2.3 Continual description

This method shows the functional dependence between stiffness and sectional internal forces:

$$S = S_0 \alpha w \quad (38)$$

where:

S_0 - initial compression, bending and shearing stiffness,

α - coefficient conditioned by the work phase of the cross-sectional area,

w - stiffness changes index.

Well known dependence for deep elements described by Ramberg-Osgood, Kuczynski has to be completed by plane stress components, i.e., compression, shearing and bending. The drop of compression, bending and shearing stiffness is determined in this method as:

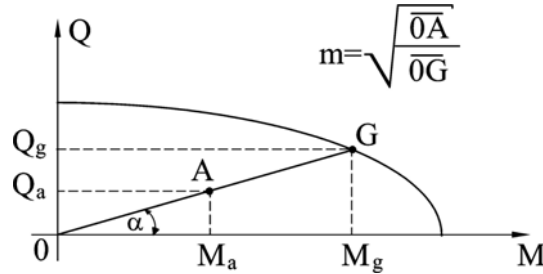


Fig. 4 The effort of the cross-sectional area

$$w = 1 - m^\psi \quad (39)$$

where:

- m - grade of the effort of the cross-section,
- ψ - cracking and concrete plasticization parameter,

The grade of the effort of the cross-section m is defined as square root of quotient of the actual effort OA and the limiting effort OG , while force N is known, Fig. 4. (M_a, Q_a – moment and force caused by actual load, M_g, Q_g – moment and force caused by limiting effort).

Mohr's destruction criterion is used to create the limiting curve in compression - shearing system.

3. Numerical tests

The numerical tests present the verification of the correctness, accuracy and efficiency of the proposed computational model of building structure.

The verification of the accuracy and efficiency of the proposed model have been done by the comparison with the analytical methods and with the results obtained by using the commercial software "DIANA" (TNO Building and Construction Research), and author's software "ORCAN" (kmb.pb.bialystok.pl/dydaktyka/tchzyz).

The results have been compared taking into account displacements, stress, internal forces, number degree of freedom, computational time and required computer memory.

3.1 Numerical test No.1

This test has allowed to estimate the correctness of the presented new finite elements according to the principals used in FEM (Zienkiewicz 1986). The convergence of displacements field in the strip elements, taking into consideration method of numerical analysis, height and width of the structure, has been examined. The 4-node and 8-node classic finite elements and presented in the paper wall and floor strip elements with linear shape function (MQDES (L)) and Hermite's shape function (MQDES (H)) have been used. Fig. 5(a) shows the analysis results obtained for the single strip, Fig. 5(b) – the results for the strips with different dimensions. Fig. 5(a) shows that application of isoparametric 8-node finite elements or MQDES(H) elements give better accuracy. The results obtained by using MQDES(H) elements were only 0.85% less accurate but the number of

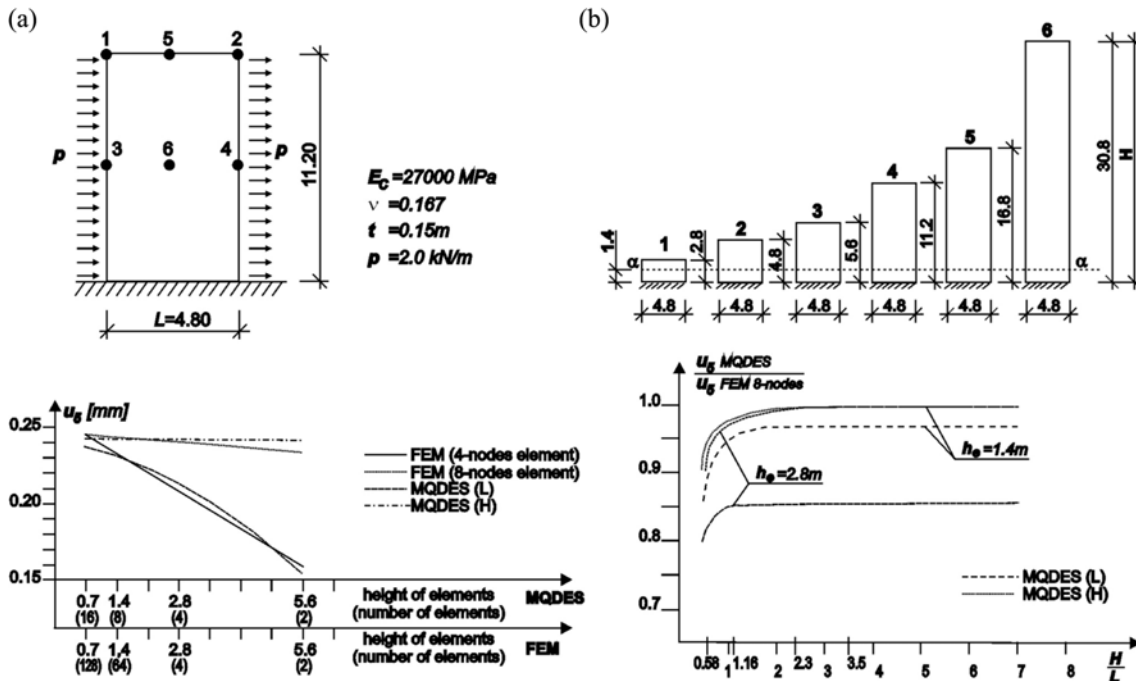


Fig. 5 Analyzed wall strip: (a) Single strip, (b) Analysed strips

unknowns have been significantly reduced (in comparison with 8-node finite elements). Fig. 5(b) proved that slenderness of structure has an influence on the results accuracy (deep elements are less accurate). For common structures the H/L ratio is greater than 2.3 and the results obtained by using MQDES(H) elements have analytical error about 1% in comparison with the results obtained by using 8-node finite elements. This test proved that MQDES(H) elements, which have height = storey of the building, can be used in proposed model.

3.2 Numerical test No.2

The test determines the values of analytical errors for the wall strip No “5” (Fig. 5b), horizontal loaded ($p = 12.085$ kN/m). The analysis has been done by using results obtained from computation carried out by methods:

- according to theory of elasticity,
- solution of Bernoulli-Euler beam (B-E),
- MQDES(H) – (height of element 2.8 m),
- FEM (8-node elements 0.6×0.7 m).

The horizontal displacements results u in wall axis (nodes 9 - 825) are shown in Table 1.

Error has been expressed by relative Euclidean norm and by relative mean error of results (displacements and stresses) obtained by proposed method and by comparative method. The results are presented in Table 2.

The obtained results show that error value is equal 1% for displacements and 2% for stresses.

Table 1 Horizontal displacements u [mm]

| Nodes | METHODS | | | |
|-------|----------------------|----------|--------|--------|
| | Theory of Elasticity | B-E beam | MQDES | FEM |
| 825 | 0.00 | 0.00 | 0.00 | 0.00 |
| 723 | 0.1420 | 0.0825 | - | 0.1417 |
| 689 | 0.2270 | 0.1430 | 0.2264 | 0.2265 |
| 621 | 0.3270 | 0.2179 | - | 0.3263 |
| 553 | 0.6997 | 0.5174 | 0.6989 | 0.6994 |
| 417 | 1.1556 | 0.9082 | - | 1.1552 |
| 383 | 1.3205 | 1.0551 | 1.318 | 1.302 |
| 315 | 1.6639 | 1.3683 | - | 1.6636 |
| 281 | 2.0200 | 1.7051 | 2.0179 | 2.0195 |
| 179 | 2.3823 | 2.0604 | - | 2.3822 |
| 145 | 2.7474 | 2.4332 | 2.745 | 2.7474 |
| 111 | 2.9300 | 2.6251 | - | 2.9300 |
| 9 | 3.4741 | 3.2240 | 3.444 | 3.4741 |

Table 2 Error values comparison

| Error type | | Compared methods | | Error values | |
|-----------------------------|-----------------------|------------------|-------|--------------|--|
| | | T. of Elast. | MQDES | FEM-MQDES | |
| Displacement of top edge | Euclidean norm [%] | u | 0.70 | 0.73 | |
| | | w | 0.12 | 0.40 | |
| | Mean error [%] | u | 0.78 | 0.90 | |
| | | w | 0.20 | 0.50 | |
| Axis displacement | Euclidean norm [%] | u | 0.32 | 0.30 | |
| | | w | 0.16 | 0.35 | |
| | Mean error [%] | u | 0.37 | 0.35 | |
| | | w | 0.20 | 0.40 | |
| Shield stresses | Euclidean norm [%] | σ_z | 1.42 | 1.02 | |
| | Mean error [%] | σ_z | 1.67 | 1.15 | |

3.3 Numerical test No.3

Test No.3 concerns the single segment of the 11-storey building (large-panel building technology). Concrete of B-20 class (according to polish standards and C16/20 according to EC2) has been used for walls and floors of 14 cm thickness. Fig. 6(a) shows computer model of the building which consists of elements proposed in the paper, Fig. 6(b) - horizontal projection of the segment.

The static and dynamic numerical analysis have been carried out by using author's software "ORCAN" and commercial software "DIANA".

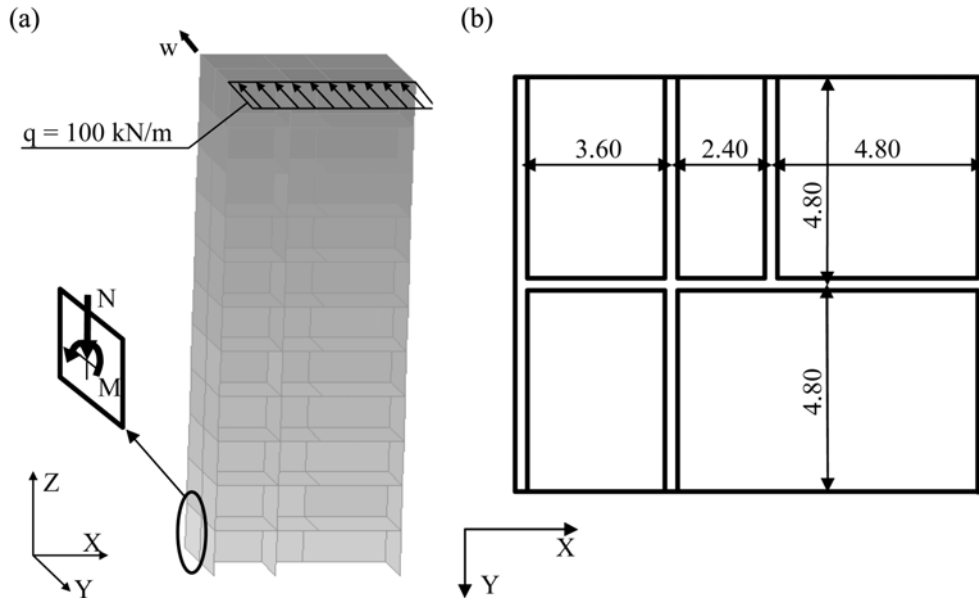


Fig. 6 Segment model: (a) Computational model, (b) Horizontal projection

Static analysis has been carried out taking into account:

- displacement in Y direction of top of the building w (Fig. 6a)
- vertical force in half-height of the lowest storey N (Fig. 6a)
- bending moment in half-height of the lowest storey M (Fig. 6a)

Fig. 7 presents the static analysis results:

- MQDES(H) - analysis has been carried out by using "ORCAN" and elements presented in the paper. Discretization system corresponds to the natural division of the building structure into wall and floor elements,
- ORCAN - analysis has been carried out by using "ORCAN" with 4-node shell elements and 4-node plane elements. Test has been done with mesh concentration 2, 4 and 10 times in both plane directions in comparison with the natural division (Fig. 7).
- DIANA - analysis has been carried out by using "DIANA" commercial software. Test has been done with mesh concentration 4 and 10 times in both plane directions in comparison with the natural division (Fig. 7).

Fig. 7 shows that the natural division of the building structure into wall and floor elements gives good solution. Mesh created by the classic finite elements had to be more concentrated to receive comparative solution. The analytical error is equal 3% in comparison with the exact solution what is caused by using Timoshenko-beam theory for the system description.

Table 3 shows some of the computational parameters of the system. It is easy to notice that proposed method gives less number of unknowns and requires less computer memory in comparison with classic FEM.

The dynamic analysis of structure has included:

- the verification of the mapping correctness of the frequency and forms of the free vibration,
- the dynamic response of the building under paraseismic impact load.

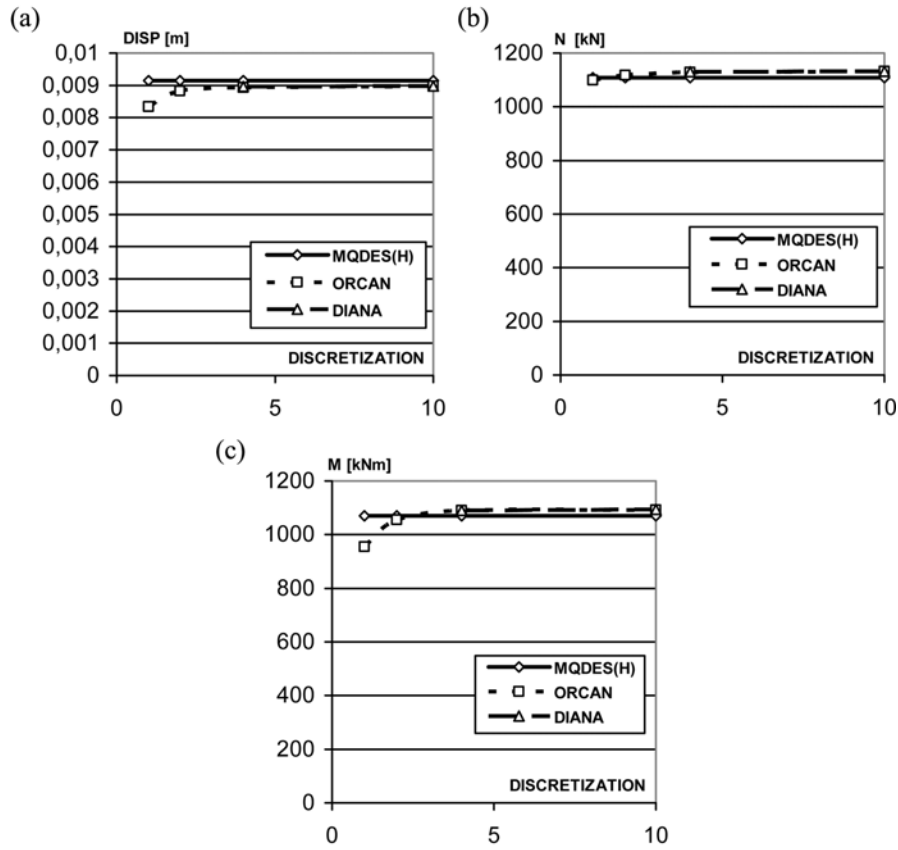


Fig. 7 Static analysis results: (a) Displacements of the building top w , (b) Strip vertical forces N , (c) Strip bending moments M

Table 3 Computational parameters (test No.3)

| Method division | | Nodes number | Elements number | Max. half band width | Computer memory |
|-----------------|----|--------------|-----------------|----------------------|-----------------|
| 1 | 2 | 3 | 4 | 5 | |
| MQDES(H) | 1 | 143 | 176 | 63 | 108 kB |
| ORCAN | 1 | 143 | 176 | 123 | 308 kB |
| | 2 | 637 | 704 | 456 | 2335 kB |
| | 4 | 2681 | 2816 | 1521 | 15.7 MB |
| DIANA | 10 | 17261 | 17600 | 5160 | 233,3 MB |
| | 4 | 2681 | 2816 | - | - |
| | 10 | 17261 | 17600 | - | - |

Fig. 8 shows three forms of vibrations. The values of free vibration frequency are presented in Table 4. Diagonal stiffness matrix has been used in computations.

The results show that proposed model which used MQDES elements can map free vibration

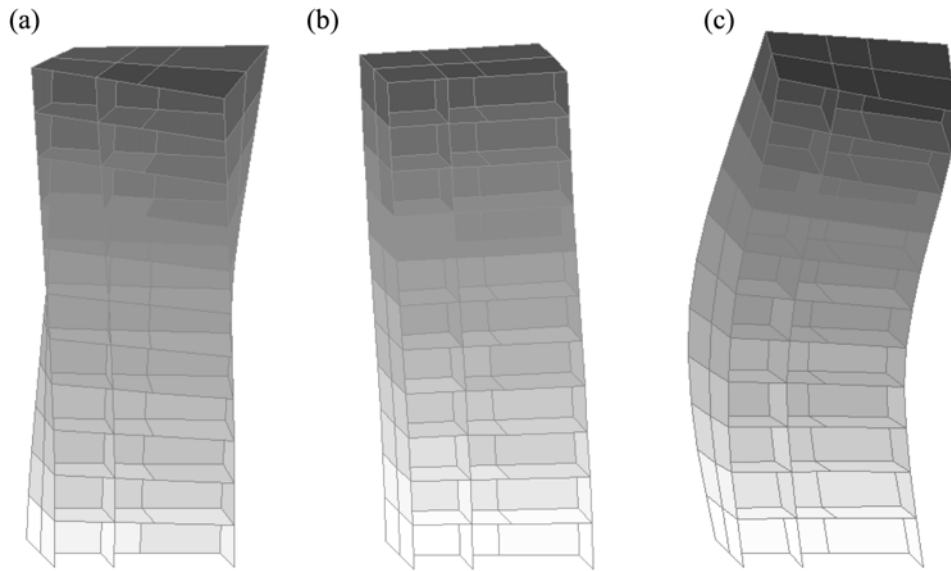


Fig. 8 Free vibration forms: (a) Torsional vibration form, (b) First free vibration form in longitudinal direction (c) Second vibration form in longitudinal direction

Table 4 Free vibration frequencies [rad/s]

| Method | division | torsional vibration frequency | I vibration frequency | II vibration frequency | Max. vibration frequency |
|----------|----------|-------------------------------|-----------------------|------------------------|--------------------------|
| | 1 | 2 | 3 | 4 | 5 |
| MQDES(H) | 1 | 14.41 | 21.96 | 71.80 | 1595.0 |
| DIANA | 2 | 15.03 | 21.80 | 71.75 | - |
| | 4 | 14.87 | 21.76 | 71.27 | - |

frequency correctly.

The dynamic response of the building segment has been tested under paraseismic impact load which had been registered on mining area of industrial complex KGHM “Polska Miedz” in Polkowice (Poland). Fig. 9 shows the accelerogram. The kinematic force used in the analysis corresponds with the results obtained from the measurements of the building foundation. The force direction is in Y axis (Fig. 6a).

Fig. 10 shows the response in the form of displacements w of segment top (without damping). The denotations ORKAN-1, -2, -4 concern the mesh concentration by using classic shield-plate finite elements what correspond with the division into 1, 4 and 16 elements in comparison with the natural division into wall or floor elements.

Table 5 presents computational times of the analysis, where:

- Newmark method has been used for the integration of motion equations and the elements stiffness matrices have been determined in every time step,
- damping has been omitted,

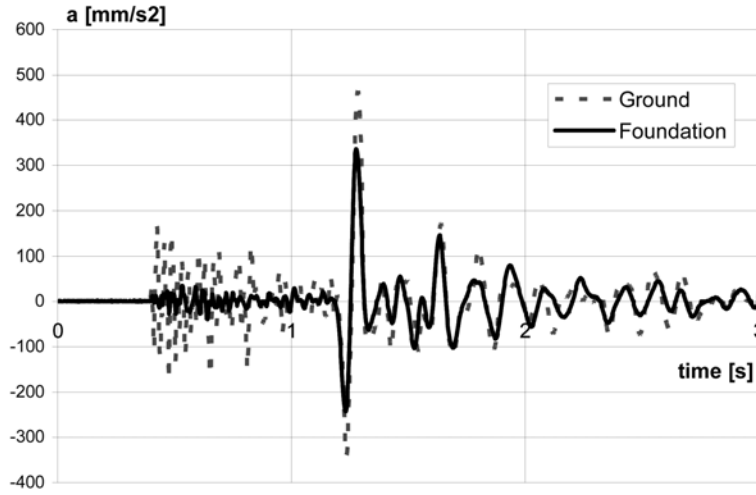


Fig. 9 Acceleration diagram – Polkowice 13.01.2000

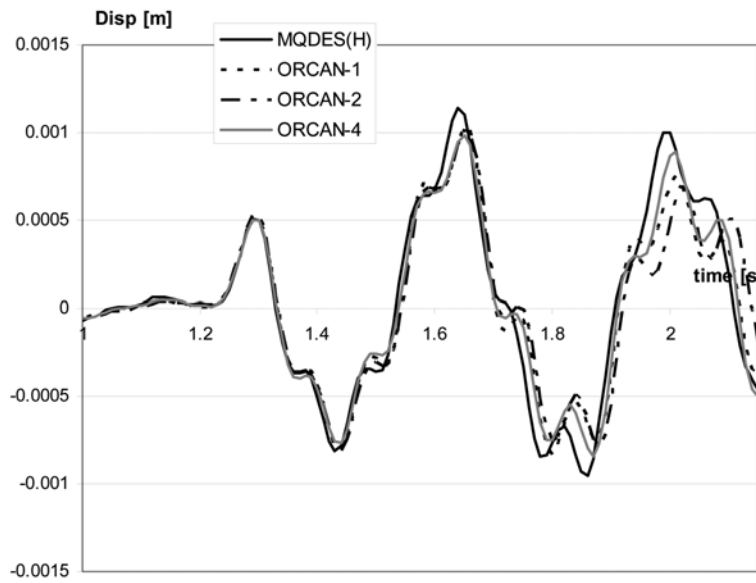


Fig. 10 Displacements diagram of the top of the segment in *w* direction

Table 5 Analysis of computational times (test No.3)

| Method division | | Computational time [s] |
|-----------------|---|------------------------|
| 1 | | 2 |
| MQDES | 1 | 70 |
| ORCAN | 1 | 930 |
| | 2 | 3727 |
| | 4 | 14889 |

- number of integration steps NSTEP = 1500,
- shield-plate elements have been integrated numerically: Gauss points number - 3×3 , number of degree of freedom - 20.

This test shows that proposed model which used MQDES elements can well describe dynamic response of the building and can provide accurate results with significantly reduced computational time.

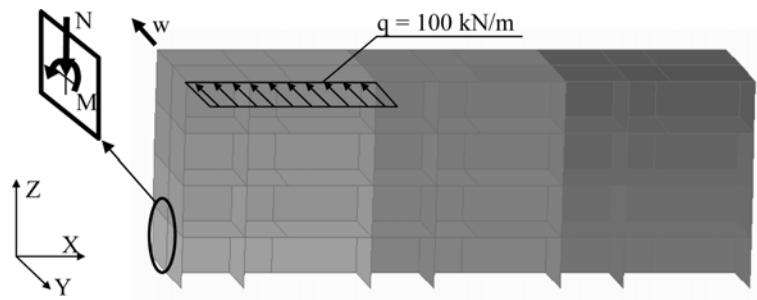


Fig. 11 Model of the building

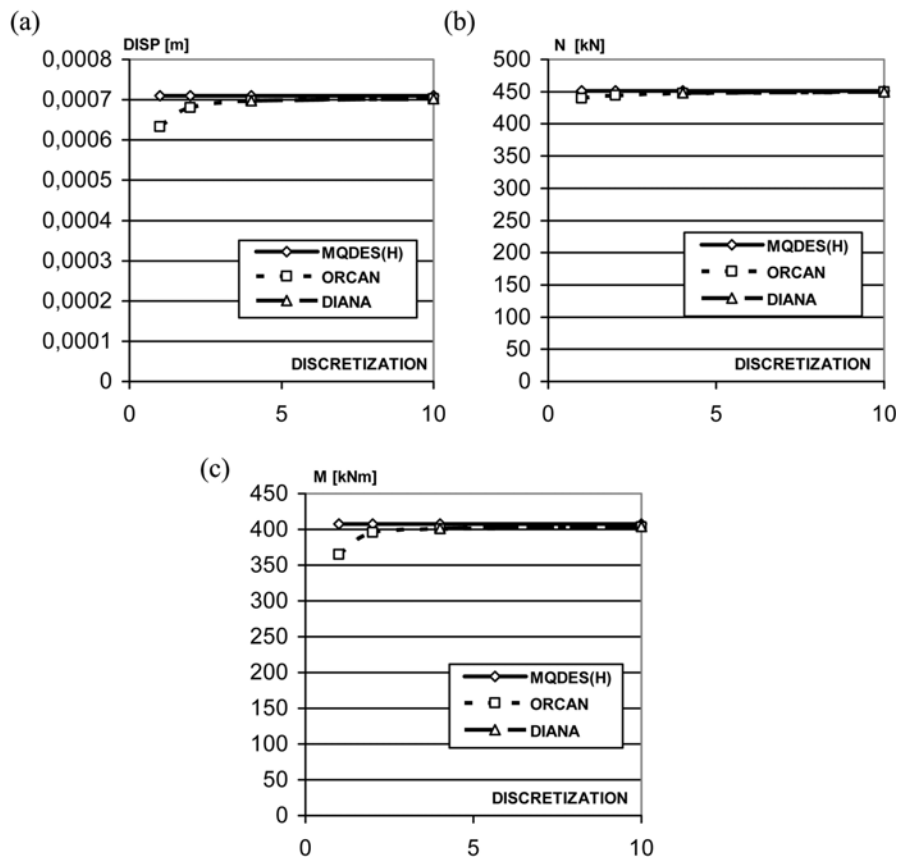


Fig. 12 Static analysis results: (a) Displacements of the building top w , (b) Strip vertical forces N , (c) Strip bending moments M

3.4 Numerical test No.4

Fig. 11 shows the 4-storey building erected in the same technology as structure showed in test No.3. The building consists of three identical segments. Fig. 6(b) presents the horizontal projection of the individual segment.

The static and dynamic numerical analyses have been carried out by using author's software "ORCAN" and commercial software "DIANA".

Static analysis has been done taking into account displacements w , vertical forces N and bending moments M (Fig. 11).

Fig. 12 presents the static analysis results (the descriptions are the same as in the test No.3).

The natural division of the building structure into wall and floor elements gives good solution.

Table 6 shows some of the computational parameters of the system. 5-th column presents the computer memory which has been required to create global matrix of the system. It is easy to notice that proposed method gives less number of unknowns and requires less computer memory in comparison with classic FEM.

The dynamic response of the building has been tested under paraseismic impact load showed in Fig. 9. The force direction is in Y axis (Fig. 11).

Table 6 Computational parameters (test No.4)

| Method | Method division | Nodes number | Elements number | Max. half band width | Computer memory |
|--------|-----------------|--------------|-----------------|----------------------|-----------------|
| | 1 | 2 | 3 | 4 | 5 |
| MQDES | 1 | 147 | 176 | 96 | 105 kB |
| ORCAN | 1 | 147 | 176 | 192 | 404 kB |
| | 2 | 645 | 704 | 705 | 3064 kB |
| | 4 | 2697 | 2816 | 2361 | 23.16 MB |
| | 10 | 17301 | 17600 | 7929 | 367,9 MB |
| DIANA | 4 | 2697 | 2816 | - | - |
| | 10 | 17301 | 17600 | - | - |

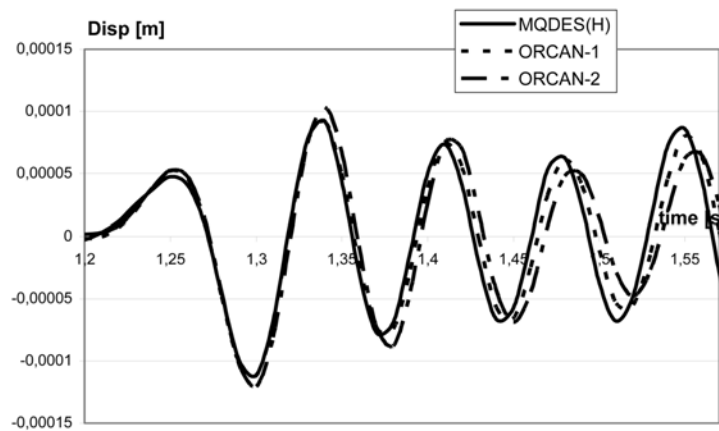


Fig. 13 Displacements diagram of the top of the building in w direction

Table 7 Analysis of computational times (test No.4)

| Method division | | Computational time [s] |
|-----------------|---|------------------------|
| 1 | | 2 |
| MQDES | 1 | 171 |
| ORCAN | 1 | 1750 |
| | 2 | 5206 |

Fig. 13 presents the response in the form of displacements w (Fig. 11) of segment top (without damping). The denotations ORKAN-1, -2 concern the mesh concentration by using classic shield-plate finite elements what correspond with the division into 1 and 4 elements in comparison with the natural division into wall or floor elements.

The computational times of the analysis are presented in Table 7.

This test proved that proposed model which used MQDES elements can well describe dynamic response of the building and can provide accurate results with significantly reduced computational time.

4. Conclusions

Presented method opens possibilities for the modelling and discretization of complex three-dimensional building structures taking into account soil-structure interaction. The model is assembled of elements corresponding to the division of a real structure into constituent elements, i.e., wall panels, floor slabs, plane and spatial joints as well as lintels. The method formulation allows in a quickly way to obtain results convergence. The accuracy of the described model depends (like in classic FEM) on the division of the structure into constituent elements. Good accuracy (about 3% - what is acceptable in engineering practice) can be obtained when the real structure is divided into its natural elements, i.e., wall panels, floor slabs etc. Because of such a division the number of unknowns is small in comparison with the number of unknowns used for structure description in classic FEM (from several to a dozens times less for the real structures). Because of the small number of unknowns the dynamic analysis of large building structures in three-dimensional scheme can be carried out easily in relative short time on commonly used hardware of PC class (the computational time is from dozens to several-hundreds times less in comparison with the commercial software). Numerical tests have confirmed the correctness and usefulness of the presented method for the analysis of complex structures subjected to kinematic force.

Proposed model can be very useful for scientific research and code verification purposes, for testing simple computational models, for structural designing in complicated load and soil conditions, for caring out expertises or for modernization existing building systems.

References

- Ali, R. and Atwall, S.J. (1980), "Prediction of natural frequencies of vibration of rectangular plates with rectangular cutouts", *Comput. Struct.*, **12**, 819-823.

- Choi, C.K. and Bang, M.S. (1987), "Plate element with cutout for perforated shear wall", *J. Struct. Eng.*, ASCE, **113**(2), 295-306.
- Choi, C.K. and Cheung, K.Y. (1996), "Three-dimensional non-conforming 8-node finite elements with rotational degrees of freedom", *Struct. Eng. Mech.*, **4**(5), 41-61.
- Choi, C.K., Kim, S.H., Park, Y.M. and Cheun, K.Y. (1998), "Two-dimensional nonconforming finite elements: A state-of-art", *Struct. Eng. Mech.*, **6**(1), 41-61.
- Choi, C.K., Lee, P.S. and Park, Y.M. (1999), "Defect-free 4-node flat shell element: NMS-4F element", *Struct. Eng. Mech.*, **8**(2), 207-231.
- Kim, H.S. and Hong, S.M. (1995), "Formulation of transition elements for the analysis of coupled wall structures", *Comput. Struct.*, **57**, 333-344.
- Kim, H.S. and Lee, D.G. (2003), "Analysis of shear wall with openings using super elements", *Eng. Struct.*, **25**, 981-991.
- Kim, H.S. and Lee, D.G. (2005), "Efficient analysis of flat slab structures subjected to lateral loads", *Eng. Struct.*, **27**, 251-263.
- Lee, D.G., Kim, H.S. and Chun, M.H. (2002), "Efficient seismic analysis of high-rise building structures with the effects of floor slabs", *Eng. Struct.*, **24**, 613-623.
- Miedzialowski, Cz. (1995), "Three-dimensional modelling of wall structures", *Archives of Civil Engineering: XLI*(2), 195-212.
- Rakowski, J. (1990), "The interpretation of the shear looking in beam elements", *Comput. Struct.*, **5**(2), 125-146.
- Thimosenko, S.P. and Goodier, J.N. (1951), *Theory of Elasticity*, McGraw-Hill, New York.
- Thomas, H. (1989), "On drilling degrees of freedom", *Comput. Meth. Appl. Mech. Eng.*, **72**, 105-121.
- Zienkiewicz, O.C. (1986), *The Finite Element Method*, McGraw-Hill.